MRS Advances © 2017 Materials Research Society
DOI: 10.1557/adv.2017.54

Energy Dispersive X-ray Diffraction (EDXRD) of $Li_{1.1}V_3O_8$ Electrochemical Cell

Qing Zhang[1], Andrea M. Bruck[2], David C. Bock[3], Jing Li[1], Eric A. Stach[4], Esther S. Takeuchi[1,2,3]*, Kenneth J. Takeuchi[1,2]*, Amy C. Marschilok[1,2]*

[1] Department of Materials Science and Chemical Engineering, Stony Brook University, Stony Brook, NY 11794
[2] Department of Chemistry, Stony Brook University, Stony Brook, NY 11794
[3] Energy Sciences Directorate, Brookhaven National Laboratory, Upton, NY 11973
[4] Center for Functional Nanomaterials, Brookhaven National Laboratory, Upton, NY 11973

*corresponding authors: (EST) esther.takeuchi@stonybrook.edu, (KJT) kenneth.takeuchi.1@stonybrook.edu, (ACM) amy.marschilok@stonybrook.edu

ABSTRACT

In this study, we conducted the first energy dispersive x-ray diffraction (EDXRD) experiments on Li/$Li_{1.1}V_3O_8$ coin cells discharged to different lithiation levels in order to investigate the phase transitions upon electrochemical reduction. The phase transformation from layered Li-poor α to Li-rich α to defect rock-salt β phase was confirmed with cells of different lithiation stages. No spatial localization of phase formation was observed throughout the cathodes under the conditions of this measurement.

INTRODUCTION

The layered material $Li_{1+n}V_3O_8$ (n=0-0.2) is recognized as an interesting cathode material for lithium based batteries, due to its high theoretical capacity (362 $mAh \cdot g^{-1}$) and power capability.(1, 2) The $Li_{1+n}V_3O_8$ structure can be viewed as a stack of V_3O_8 layers with Li^+ ions in the interlayer space. Each V_3O_8 consists of alternating edge-sharing VO_5 trigonal bi-pyramids and edge-sharing VO_6 octahedrons.(3) Upon lithiation to $Li_{\sim 2.5}V_3O_8$, the parent layered phase (Li-poor α) undergoes distortion to form the less crystalline Li-rich α while maintaining the same V_3O_8 layer structure. Upon further lithiation to $Li_{\sim 4}V_3O_8$, the layered α phase transforms to a defect-rock salt phase β. Further lithiation beyond $Li_4V_3O_8$ takes place in the β phase.(3, 4)

The transition from the α to the β phase has only been evaluated on bulk electrodes as a function of depth of discharge. To get full utilization of an active material in the electrode, homogeneous discharge is critical where the phase transition occurs evenly throughout the entire electrode. If phase transition is localized, it could prevent full utilization of the active material and result in lower delivered capacity. Therefore, a composite electrode must have a full percolation network to allow for good electron conduction, while the active material retains good intrinsic Li^+ conductivity. Energy dispersive x-ray diffraction (EDXRD) uses high energy X-rays that can penetrate the steel casing of a coin cell and record XRD patterns as a function of spatial location in the cell. Recent studies by Kirshenbaum et al. have shown a rate dependence on the homogeneity of discharge of the $Ag_2VP_2O_8$ material, a bimetallic, layered cathode material.(5) The reduction of Ag^+ to Ag^0 was an indicator of discharge homogeneity with more localized Ag^0 formation taking place at a high C rate (C/168) while a slower C-rate (C/1440) allowed for even Ag^0 distribution throughout the electrode.(6) Gallaway et al. observed a similar trend in the Zn/MnO_2 alkaline battery system with the cathode conversion reaction of MnO_2 to Mn_3O_4 at

different C rates, and the formation of new phase and with a different distribution.(7) Other examples of heterogeneous discharge observed at different C rates include $LiMn_2O_4$ based spinel material and $LiFePO_4$ tunneled materials.(8-10) All of these studies highlighted the detrimental effects of capacity loss that heterogeneous discharge can have on the performance of the electrochemical cell. Our EDXRD study reported here is the first to evaluate the discharge of $Li_{1.1}V_3O_8$ material with spatial resolution.

Experimental

Material synthesis and electrode preparation

The $Li_{1.1}V_3O_8$ sample was synthesized via a sol-gel approach as reported previously.(11) Electrodes for the EDXRD test combined $Li_{1.1}V_3O_8$ powder, carbon and graphite in a weight ratio of 90:5:5 as pressed pellets.

Coin cell construction and electrochemical testing

Coin type cells with $Li_{1.1}V_3O_8$ cathode (coating or pellets), Li anode and polypropylene separator were constructed in an argon-filled glove box. 1 M $LiPF_6$ in ethylene carbonate/dimethyl carbonate (in volume ratio of 3:7) was used as electrolyte. Coin cells were cycled at C/10 rate in the voltage window of 3.8-2.0 V vs. Li/Li^+. For the EDXRD experiment, coin cells were discharged at a current rate of C/150 to several lithiation levels ($Li_{1.5}V_3O_8$, $Li_{2.5}V_3O_8$, $Li_{3.7}V_3O_8$, and $Li_{4.1}V_3O_8$). Undischarged and discharged cells will be referred to as $Li_{1.1}$, $Li_{1.5}$, $Li_{2.5}$, $Li_{3.7}$ and $Li_{4.1}$ in the following text.

Material Characterization

The angle dispersive X-ray diffraction (ADXRD) of $Li_{1.1}V_3O_8$ powder was conducted on a Rigaku Smartlab Diffractometer. Scanning electron microscope (SEM) images were acquired on a JEOL 7600 field emission microscope. Transmission electron microscope (TEM) images were acquired on a JEOL JEM 2100 instrument operating at 200 keV.

The energy dispersive X-ray diffraction (EDXRD) measurement of $Li_{1.1}V_3O_8$ coin cells was conducted at the Advanced Photon Light Source at Argonne National Laboratory on Beamline 6-BM-B. White beam radiation was focused with slits to make the final gauge volume $3.6 \times 1.0 \times 0.02$ mm. Coin cells were situated flat on the stage and the stage moved vertically in 20 μm increments to obtain the EDXRD spectra for each region inside the cell at any given (x,y) position. The germanium detector was set to 2-theta = 3°. The setup and experimental conditions have been published previously.(6) Data analysis was performed on Matlab software.

RESULTS AND DISCUSSION

ADXRD data of the $Li_{1.1}V_3O_8$ powder is shown in **Figure 1**. The diffraction peaks can be well indexed to reference PDF# 01-073-8145 with *P21/m* space group. The crystal structure of the α and β phase are shown in **Figure 2a-b**. As described before, α is a layered structure and β is a defect rock salt structure where the V and Li coordination is more symmetrical than α. The synthesized material showed rod-shape morphology, as shown in **Figure 2c-d**. The d spacing of 1.22 nm obtained from HRTEM of the lattice fringes matched well with (001) lattice planes of the $Li_{1.1}V_3O_8$ structure.

The electrochemistry of $Li_{1.1}V_3O_8$ is presented in **Figure 3a**. At the current rate of C/10, the cell delivered 245 and 257 mAh·g^{-1} on the 1st and 2nd cycle, respectively, with 219 mAh·g^{-1} maintained on the 100th cycle. For the EDXRD measurement, cells were discharged to different lithiation stages and the discharge curves are shown in **Figure 3b**. Before the voltage reaches 2.6 V, lithiation is in the parent α phase. The plateau at ~2.6 V marked the α – β transition where the two phases coexist. Below 2.6 V, lithiation is in the β phase.(3) According to the discharge curves, the $Li_{1.5}$ and $Li_{2.5}$ cell are likely to have α phase structure, while the $Li_{3.7}$ and $Li_{4.1}$ cell are likely to β phase structure.

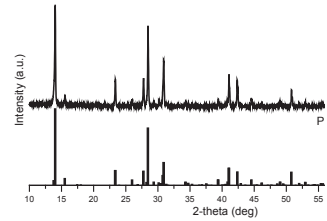

Figure 1 ADXRD of $Li_{1.1}V_3O_8$ powder with reference pattern

A raw, full EDXRD scan of the $Li_{3.7}$ cell is shown in **Figure 4** where regions of the steel casing, cathode, separators and Li anode are clearly present. In **Figure 5**, four scans from each cell (at 40, 140, 240, 340 μm from the separator) are shown to indicate the peak shifts during four stages of lithiation. The four scans across the electrode from each cell appear identical in terms of peak location and peak intensity, indicating uniform distribution of phase formation spatially. Different from the intensities in the ADXRD where the (100) peak usually gives the highest intensity, the peak intensities in the EDXRD are energy-dependent, therefore the (100) peak is difficult to resolve from the background in the regions of low intensity. With lithiation from $Li_{1.1}$ to $Li_{2.5}$, the α (003) peak shifted from 1/d= 0.262 Å towards lower 1/d value to 0.258 Å, indicating expansion of the lattice along *c* axis. The α (-111) peak moved from 1/d= 0.318 Å to 0.312 Å and α (-202) peak moved from 1/d= 0.311 Å to 0.322 Å. From Li-poor α to Li-rich α, the structure contracts along *a* axis and expands along *b* and *c* axis with constant lattice cell volume. Li-rich α is more distorted and less crystalline than the parent Li-poor α, as the structure accommodates more Li^+.(12) Upon further lithiation to $Li_{3.7}$, the (003) peak at 1/d= 0.260 Å, (-111) peak at 1/d= 0.304 Å and the (103) peak at 1/d= 0.353 Å suggest the formation

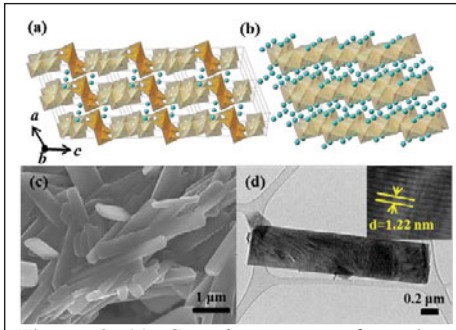

Figure 2 (a) Crystal structure of α phase $Li_{1.1}V_3O_8$; (b) Crystal structure of β phase $Li_4V_3O_8$; (c) SEM image of $Li_{1.1}V_3O_8$; and (d) TEM image of $Li_{1.1}V_3O_8$.

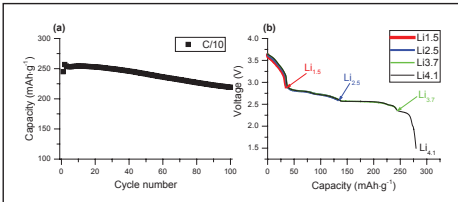

Figure 3 (a) Capacity versus cycle number of Li/$Li_{1.1}V_3O_8$ coin cells cycling at C/10. (b) Discharge curves of the coin cells prepared for the EDXRD experiment. Arrows indicated where the curves end.

of β phase. While most peaks that were attributed to α disappeared, the α (-111) peak at 0.312 Å is still visible, indicating the α-β transition has not completed as this stage. As the EDXRD experiments were conducted several days after the cells were discharged, there was opportunity for voltage relaxation. The $Li_{4.1}$ cell was found to be entirely β phase. Transforming from α to β phase, the O and Li atoms undergo small displacement to adopt a more cubic-close-packed structure.(12)

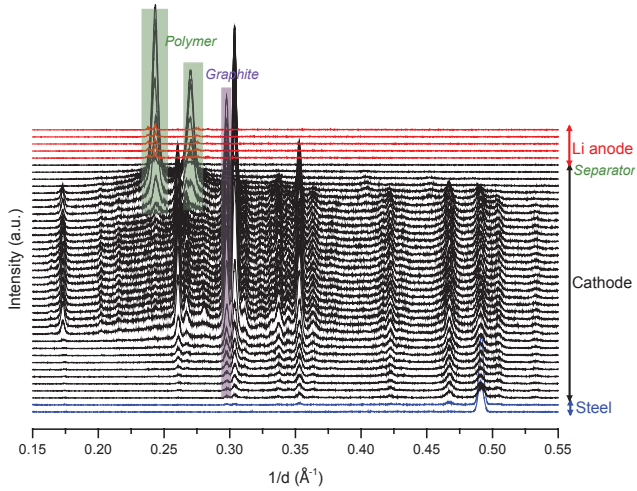

Figure 4 Full EDXRD scan of $Li_{3.7}V_3O_8$ cell.

The phase transformation observed at different lithiation stages is consistent with the *ex-situ* XRD experiment on LiV_3O_8 discharge and charge reported previously.(1)

In **Figure 6**, representative peaks for α and β phases were chosen based on highest intensity of the EDXRD spectra. The peak intensity of graphite (002) at 1/d=0.296 Å was used as a reference to monitor the regions of varying intensity resulting from attenuation. As described before, the $Li_{3.7}$ cell has mixed phases with predominantly β phase. It is clear that the intensity of the α and β peaks in the four cells remains constant with respect to the graphite (002) peak within the electrode. Under the conditions of this experiment, including the relaxation time discussed above, there was no variation of phase localization at each lithiation stage, consistent with effective utilization of the electroactive material.

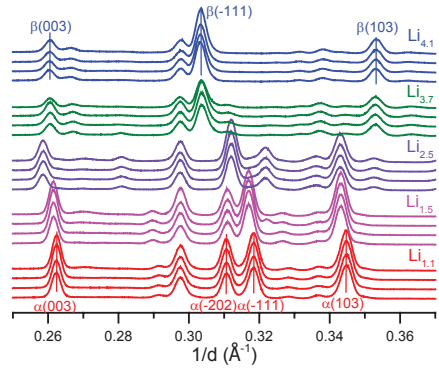

Figure 5 Four scans of each cell ($Li_{1.1}V_3O_8$, $Li_{1.5}V_3O_8$, $Li_{2.5}V_3O_8$, $Li_{3.7}V_3O_8$ and $Li_{4.1}V_3O_8$) at 40, 140, 240, and 340 μm from the separator.

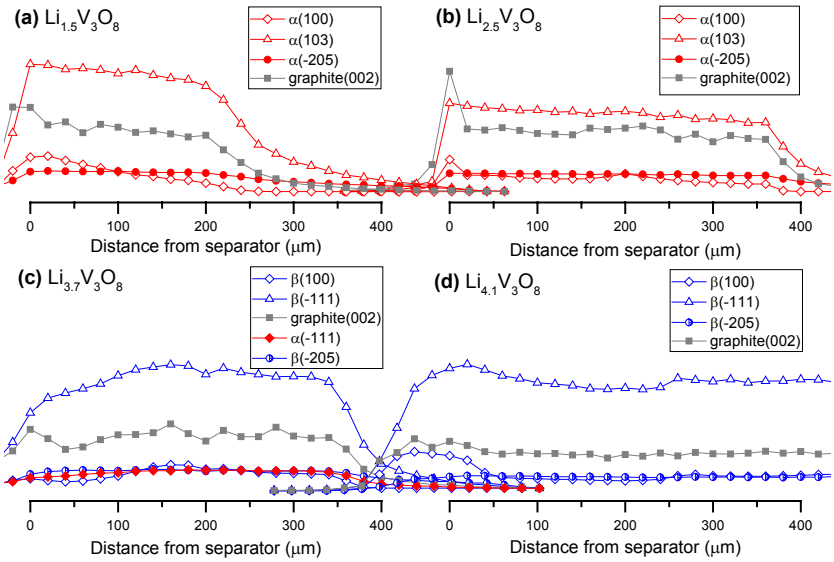

Figure 6 Intensity change of selected peaks with respect to location of the electrodes of the cells of $Li_{1.5}V_3O_8$, $Li_{2.5}V_3O_8$, $Li_{3.7}V_3O_8$ and $Li_{4.1}V_3O_8$.

CONCLUSIONS

In this study, phase transition and Li diffusion throughout the $Li_{1.1}V_3O_8$ electrode were elucidated through the use of EDXRD. An undischarged $Li_{1.1}V_3O_8$ cell and four cells discharged to different lithiation levels were analyzed after several days of relaxation. The phase transformation from layered Li-poor α phase to Li-rich α phase with lithiation to $Li_{2.5}V_3O_8$, and the transformation from α phase to defect rock-salt β phase with lithiation further to $Li_{4.1}V_3O_8$ was demonstrated. No spatial localization of phase formation was found throughout the electrodes under these conditions. EDXRD proved to be a useful means to study the structure evolution of $Li_{1.1}V_3O_8$ material during lithiation and de-lithiation, and the findings in this report contribute to more fully understanding the functional capacity of $Li_{1.1}V_3O_8$. Localized phase formation could prevent full utilization of active material and give rise to loss of functional capacity. This study lays the groundwork for future *in-situ* and *operando* experiments which could further assess the ability of $Li_{1.1}V_3O_8$ material to homogeneously discharge**.**

ACKNOWLEDGMENTS

This work was supported as part of the Center for Mesoscale Transport Properties, an Energy Frontier Research Center supported by the U.S. Department of Energy, Office of Science, Basic Energy Sciences, under award #DE-SC0012673 for financial support. This research used

resources of the Advanced Photon Source beamlines 6-BM B, a U.S. Department of Energy (DOE) Office of Science User Facility operated for the DOE Office of Science by Argonne National Laboratory under Contract No. DE-AC02-06CH113. Use of APS Beamline 6-BM is partially supported by the National Synchrotron Light Source II, Brookhaven National Laboratory, under DOE Contract No. DE-SC0012704. Transmission electron microscopy at Brookhaven National Laboratory used resources of the Center for Functional Nanomaterials, which is a US DOE Office of Science Facility, at Brookhaven National Laboratory under Contract No. DE-SC0012704.

REFERENCES

1. S. Sarkar, A. Bhowmik, M. Dixit Bharadwaj and S. Mitra, *J. Electrochem. Soc* **161**, A14 (2014).

2. Q. Shi, J. W. Liu, R. Z. Hu, M. Q. Zeng, M. J. Dai and M. Zhu, *RSC Adv.*, **2**, 7273 (2012).

3. L. A. de Picciotto, K. T. Adendorff, D. C. Liles and M. M. Thackeray, *Solid State Ion*. **62**, 297 (1993).

4. G. Pistoia, S. Panero, M. Tocci, R. V. Moshtev and V. Manev, *Solid State Ion*. **13**, 311 (1984).

5. K. Kirshenbaum, D. C. Bock, C.-Y. Lee, Z. Zhong, K. J. Takeuchi, A. C. Marschilok and E. S. Takeuchi, *Science*, **347**, 149 (2015).

6. K. C. Kirshenbaum, D. C. Bock, A. B. Brady, A. C. Marschilok, K. J. Takeuchi and E. S. Takeuchi, *Phys. Chem. Chem. Phys.* **17**, 11204 (2015).

7. J. W. Gallaway, M. Menard, B. Hertzberg, Z. Zhong, M. Croft, L. A. Sviridov, D. E. Turney, S. Banerjee, D. A. Steingart and C. K. Erdonmez, *J. Electrochem. Soc* **162**, A162 (2015).

8. G. Liang, M. Croft and Z. Zhong, *ECS Trans.* **50**, 293 (2013).

9. W. A. Paxton, Z. Zhong and T. Tsakalakos, *J. Power Sources* **275**, 429 (2015).

10. F. C. Strobridge, B. Orvananos, M. Croft, H.-C. Yu, R. Robert, H. Liu, Z. Zhong, T. Connolley, M. Drakopoulos, K. Thornton and C. P. Grey, *Chem. Mater.* **27**, 2374 (2015).

11. A. C. Marschilok, C. P. Schaffer, K. J. Takeuchi and E. S. Takeuchi, *J. Compos. Mater.* **47**, 41 (2013).

12. S. Jouanneau, A. Verbaere and D. Guyomard, *J. Solid State Chem.* **178**, 22 (2005).